A strikingly ornamented fossil alligator lizard (Squamata: *Abronia*) from the Miocene of California

SIMON G. SCARPETTA[1,*,©] and DAVID T. LEDESMA[2]

[1]*Museum of Vertebrate Zoology, University of California Berkeley, 3101 UC Berkeley Road, Berkeley, CA 94720, USA*
[2]*Department of Integrative Biology, The University of Texas at Austin, Austin, TX 78712, USA*

Extant alligator lizards of the genus *Abronia* are found in montane cloud forests and pine-oak forests of Mesoamerica and are iconic among the public and scientific communities. Here, we describe a fossilized partial skull from the Miocene of southern California (~12.5–11.0 Mya) that is the first definitive fossil and only recognized extinct species of *Abronia*. The locality of the fossil is substantially removed from the range of extant species of *Abronia*. This remarkable biogeographical discovery corroborates previous speculation that *Abronia* was distributed north of Mexico during the Neogene, a scenario that could not be inferred from the geographical ranges and phylogeny of the extant species alone. Additionally, the fossil preserves a distinctive morphology, osteoderm sails, that appears unique to the new taxon among alligator lizards. The finding emphasizes the importance of the fossil record for historical biogeography and could motivate new avenues of biogeographical research in Mesoamerica and the USA.

ADDITIONAL KEYWORDS: Anguidae – biogeography – new species – osteoderm morphology – palaeontology – phylogenetics – taxonomy.

INTRODUCTION

Alligator lizards of the genus *Abronia* Gray, 1838 (Anguidae: Gerrhonotinae) are known for their impressive physical appearance and restricted distributions in montane forests of Mesoamerica (Campbell & Frost, 1993). *Abronia* are increasingly recognized as conservation flagship taxa (Clause *et al.*, 2020). There are 41 recognized species of *Abronia* (Solano-Zavaleta & Nieto-Montes de Oca, 2018; García-Vázquez *et al.*, 2022), and many of these are threatened or endangered (IUCN, 2022).

Recently, phylogenomic analyses of a double-digest restriction site-associated DNA sequencing (ddRADSeq) dataset revealed widespread paraphyly between *Abronia* and the formerly recognized genus *Mesaspis* Cope, 1878; hence, ten terrestrial species of alligator lizard previously accommodated in *Mesaspis* were placed in *Abronia* (Gutiérrez-Rodríguez *et al.*,

2021). In that study, eight of 11 putative subclades of *Abronia* were sampled and provided a well-supported phylogeny, with a basal divergence between species found west of the Isthmus of Tehuantepec and those found east of the Isthmus (Fig. 1A; Gutiérrez-Rodríguez *et al.*, 2021). Thus, arboreal and terrestrial life histories and morphotypes that were traditionally associated with *Abronia* and *Mesaspis*, respectively, have evolved multiple times (Good, 1987; Campbell & Frost, 1993). *Abronia*, especially the arboreal species, have limited and often allopatric distributions in montane cloud forests and seasonally dry pine-oak forests (Campbell & Frost, 1993; Solano-Zavaleta & Nieto-Montes de Oca, 2018; Gutiérrez-Rodríguez *et al.*, 2021). Based on modern species ranges, the crown clade presumably had a restricted distribution in Mesoamerica throughout its history. Published divergence time analyses suggest a late Oligocene to early Miocene origin for crown *Abronia* (24–23 Mya) and a late Oligocene divergence between *Abronia* and its sister taxon, *Barisia* Gray, 1838 (25 Mya) (Zheng & Wiens, 2016; Blair *et al.*, 2022).

Given the geographical and ecological restriction of many *Abronia* to environments not conducive to the fossilization process, it is not surprising that there are

*Corresponding author. scas100@berkeley.edu
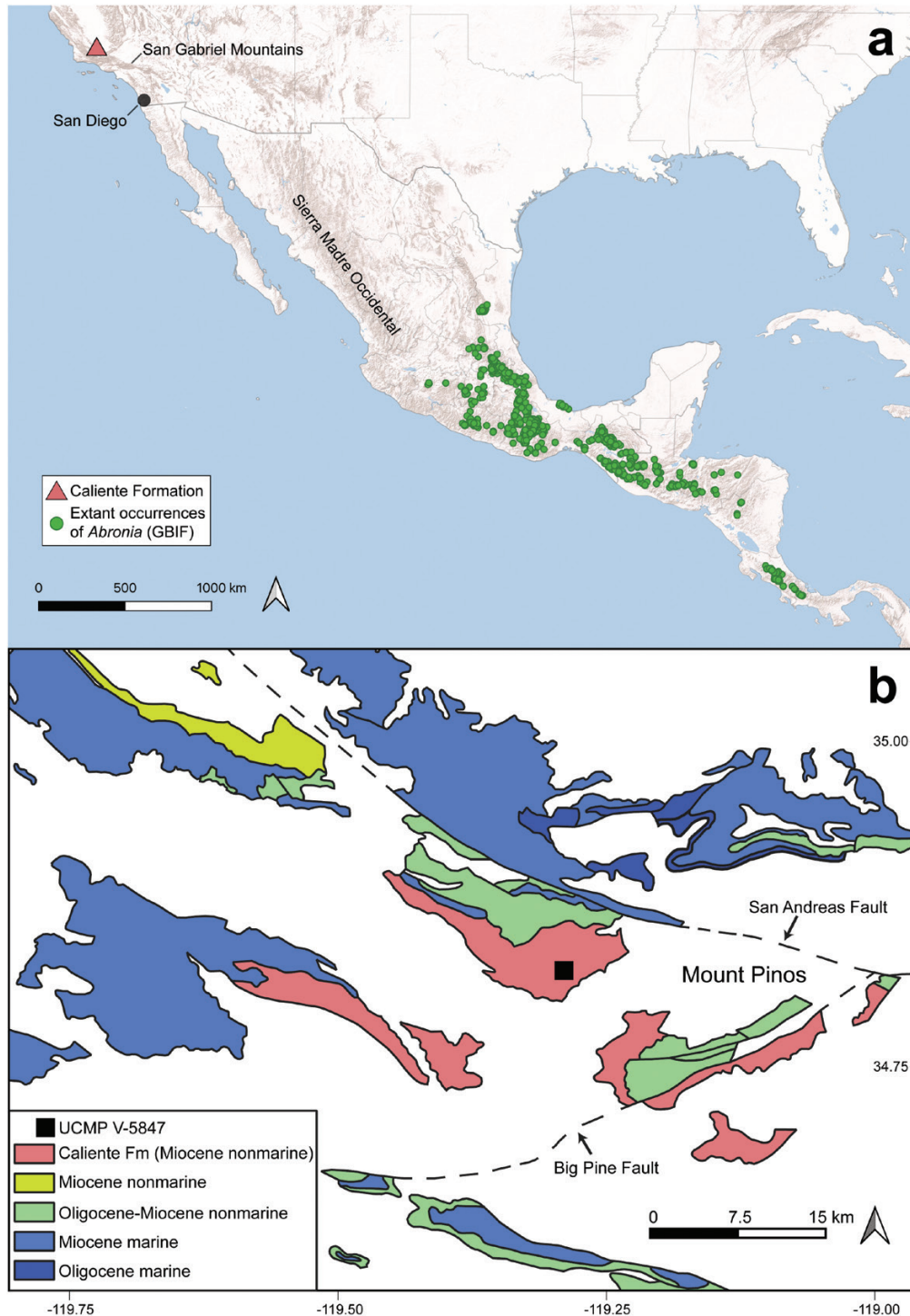
Figure 1. A, geographical context. B, local Oligocene and Miocene sedimentary units. In A, distribution data for *Abronia* are from GBIF.org (2021). Distribution data were filtered manually to remove selected outliers using the study by Gutiérrez-Rodríguez *et al.* (2021) as a reference. Grey shading in A indicates elevation (i.e. mountainous areas). Geological data in B are based on the studies by Hoyt *et al.* (2018) and Jennings (2010). The location of the *UCMP V-5847* fossiliferous site was obtained from the study by James (1963).

no formally recognized fossils of *Abronia*. The earliest fossil gerrhonotines identified with apomorphies are reported from the early Eocene (Smith, 2009). Several extinct gerrhonotines from the late Neogene of the USA (*Paragerrhonotus ricardensis* Estes, 1963, *Gerrhonotus mungerorum* Wilson, 1968 and *Elgaria peludoverde* Scarpetta, Ledesma & Bell, 2021) were hypothesized to be part of or closely related to *Abronia* (Good, 1985, 1988a; Norell, 1989), and thus the possibility and potential ramifications of extralimital occurrences of *Abronia* have been discussed previously. However, those fossils are referrable to other gerrhonotine genera (*E. peludoverde*; Scarpetta *et al.*, 2021) or are of uncertain systematic affinity (*P. ricardensis* and *G. mungerorum*; see Good, 1985, 1988a; Conrad & Norell, 2008; Norell *et al.*, 2008). Most previously described fossil alligator lizards were referred to the genera *Elgaria* Blainville, 1835 or *Gerrhonotus* Wiegmann, 1828 (Estes, 1983; Scarpetta, 2018; Scarpetta *et al.*, 2021), which occur in the USA, Mexico and Canada (Leavitt *et al.*, 2017; García-Vázquez *et al.*, 2018).

Here, we describe a fossilized partial skull that is the first definitive fossil of *Abronia* and that represents the only described extinct species of *Abronia*. The fossil is from the Miocene Caliente Formation of California. This discovery suggests a different biogeographical scenario for *Abronia* than do the distributions of the extant species and confirms the almost 40-year-old hypothesis that *Abronia* once occurred in what is now the USA (Good, 1985). The fossil is armoured with heavily ornamented osteoderms and possesses a distinctive osteoderm morphology that is unique among observed alligator lizards.

MATERIAL AND METHODS

GEOLOGICAL AND ENVIRONMENTAL SETTING

The Caliente Formation lies in the Cuyama Valley Badlands in southern California. The formation contains non-marine sediments of fluvial and lacustrine origin (Ehlert, 2003) that occasionally interfinger with marine rocks (Fig. 1B; James, 1963; Prothero *et al.*, 2008; Jennings, 2010; Hoyt *et al.*, 2018). The formation is broadly split into a lower grey-bed lithofacies and an upper red-bed lithofacies (James, 1963). A sediment provenance study determined that source rocks were derived from local sources, including the San Gabriel Mountains, and that the Caliente formation is a vestige of a drainage system confined by the ancestral San Gabriel Mountains and Sierra Pelona (Hoyt *et al.*, 2018). Slip along the San Gabriel, Canton and San Andreas faults, concurrent with and after deposition, indicates that the Caliente Formation was located up to several hundred kilometres south of its current location during the middle to late Miocene,

closer to the modern latitude of San Diego (Blakey & Ranney, 2018; Hoyt, 2018).

The fossil, *UCMP 54560*, was collected at University of California Museum of Paleontology (UCMP) V-5847 or 'Big Cat Quarry,' a fossiliferous site in red-brown calcareous mudstone beds of the Apache Canyon sequence in the red-bed (upper) lithofacies (James, 1963). University of California Museum of Paleontology V-5847 contains several aggregates of small vertebrates, some of which were interpreted as owl pellets disarticulated by flowing water (James, 1963). Taxa reported from *UCMP V-5847* include passeriform birds, sciurid rodents, lagomorphs, shrews, a carnivoran, a gomphothere, an artiodactyl, a bat and '*Gerrhonotus*' (James, 1963). The gerrhonotine fossil described here is the skull mentioned, but not formally described, by James (1963). No other lizard taxa were mentioned by James (1963), but other fossil lizards from the Caliente Formation exist and have been assigned preliminarily to Phrynosomatidae (S. Scarpetta, unpublished data).

Based on several mammals (e.g. hedgehogs and flying squirrels), the Caliente Formation was interpreted as a subtropical refugium (James, 1963). However, the identifications of several taxa that were reported to indicate a subtropical environment were later questioned based on morphological data from extant comparative material (e.g. Thorington *et al.*, 2005). The only plant fossils described from the Caliente Formation are *Celtis* L. (hackberry; Cannabaceae) (James, 1963). Palaeofloral assemblages from the adjacent but inland Mint Canyon Formation, which shares source rocks with the Caliente Formation (Hoyt *et al.*, 2018) and was deposited roughly contemporaneously, contain species consistent with a semi-arid oak woodland and savanna similar to modern ecosystems in the Sierra Madre Occidental (SMO) of northern Mexico and southern Arizona (Axelrod, 1940, 1979). University of California Museum of Paleontology V-5847 is near the coordinates 34.814°N, 119.285°W, and the modern elevation of the locality is ~1440 m (Google Earth Pro, 2021).

TEMPORAL CONSTRAINT

The grey-beds (lower lithofacies) of the Caliente Formation were dated to 15.2 Mya using the K-Ar dating method (Evernden *et al.*, 1964). Fossil mammals at *UCMP V-5847* and adjacent localities are indicative of the Clarendonian North American Land Mammal Age (~12.5–9.4 Mya; Tedford *et al.*, 2004; Barnosky *et al.*, 2014). Palaeomagnetic analysis and fossils from the Apache Canyon sequence from which *UCMP 54560* was collected established a correlation of the magnetozones in Apache Canyon with chrons C5An–C5r, corresponding to 12.47–11.06 Mya (Prothero *et al.*, 2008; Raffi *et al.*, 2020), thus establishing an age range for *UCMP 54560*.

ANATOMICAL TERMINOLOGY AND INSTITUTIONAL ABBREVIATIONS

Terminology follows Evans (2008) unless otherwise noted.

Abbreviations: FMNH, Field Museum of Natural History, Chicago, IL, USA; MVZ, Museum of Vertebrate Zoology, Berkeley, CA, USA; SDNHM, San Diego Museum of Natural History, San Diego, CA, USA; TCWC, The Texas A&M Biodiversity Research and Teaching Collections, College Station, TX, USA; TNHC, Biodiversity Collections, The University of Texas at Austin, Austin, TX, USA; UCMP, University of California Museum of Paleontology, Berkeley, CA, USA; UF, Florida Museum of Natural History, Herpetology Division, University of Florida, Gainesville, FL, USA; UTA, University of Texas at Arlington Herpetological Collections, Arlington, TX, USA.

HIGH-RESOLUTION X-RAY COMPUTED TOMOGRAPHY

We used high-resolution X-ray computed tomography (CT) to visualize *UCMP 54560*. We scanned the articulated partial skull and most of a block of red mudstone containing other cranial elements at The University of Texas at Austin High-Resolution X-ray Computed Tomography Facility on a high-resolution NSI scanner with a Fein Focus high-power source. The slice dataset for the skull consists of 1834 16-bit TIFF slices in the *x–y* plane, and the dataset for the block consists of 1845 slices. The voxel slice for both scans is 0.00966 mm. We visualized and digitally segmented the slices using the AVIZO LITE v.8.1 and v.9.3 software, using manual selections and the magic wand tool with greyscale values between 24 000 and 30 000. Many of the elements were difficult to separate digitally from the matrix; therefore, we did not segment them.

PHYLOGENETIC ANALYSES AND CHARACTER SCORES

We scored *UCMP 54560* for the specimen-based phylogenetic matrix created by Scarpetta *et al.* (2021) to assess systematics of extant and extinct alligator lizards. The matrix is composed of 80 characters and contains 25 species and 42 specimens of extant gerrhonotines. We reassessed character states for continuous morphological features binned using automation by Scarpetta *et al.* (2021) using the code from that study; all state values remained the same. We assessed the width of the facial process of the maxilla using tooth counts of the left maxilla provided by Scarpetta *et al.* (2021). The left maxilla of *UCMP 54560* has two fewer teeth than the right maxilla, and the orbital process of the left maxilla appears incomplete. Thus, the relative width of the facial process of the left maxilla is likely to be overestimated. Regardless, the facial process was placed by the binning analysis

in the 'narrow' state that is typical of several species of *Abronia*. Likewise, the length of the frontal was probably overestimated, because the two large pieces of the frontal are slightly separated. Nevertheless, the frontal was placed in the 'wide' character state.

We conducted Bayesian analyses in MrBayes v.3.2.7 (Ronquist *et al.*, 2012). Analyses consisted of two runs of 2 000 000 generations, each with four Markov chain Monte Carlo chains, sampling every 1000 generations. We set the symmetric dirichlet hyperprior at infinity and character coding (lset command) to variable. We visualized results in TRACER v.1.7 (Rambaut *et al.*, 2018) to ascertain convergence (effective sample size values > 200 for all model parameters for each run) and summarized trees as 50% majority-rule consensus trees (sumt command). We conducted parsimony analyses in PAUP v.4.0 (Swofford, 2003) using a heuristic search, 10 000 replicates, multistate codings treated as polymorphic and random taxon addition. We summarized the results as strict consensus trees and treated all characters in all analyses as unordered and equally weighted. Summary statistics for parsimony analyses are in Supporting Information, Table S1.

We performed unconstrained and fully or partially constrained analyses (i.e. with molecular scaffolds). For fully constrained analyses, relationships between *Abronia*, *Barisia* Gray, 1838, *Elgaria* Gray, 1838 and *Gerrhonotus* Wiegmann, 1828 followed Blair *et al.* (2022), those among *Abronia* followed Gutiérrez-Rodríguez *et al.* (2021), those of *Elgaria* followed Leavitt *et al.* (2017), and relationships among *Gerrhonotus* were based on the study by García-Vázquez *et al.* (2018). *Abronia ornelasi* Campbell, 1984, *Desertum lugoi* McCoy, 1970 (generic assignment *sensu* Blair *et al.*, 2022) and *Gerrhonotus parvus* Knight & Scudday, 1985 were excluded from *Elgaria*, but otherwise could attach anywhere on the tree. Partially constrained analyses constrained all aforementioned relationships except those among *Abronia*.

RESULTS

SYSTEMATIC PALAEONTOLOGY

SQUAMATA OPPEL, 1811

ANGUIMORPHA FÜRBRINGER, 1900

ANGUIDAE GRAY, 1825

GERRHONOTINAE TIHEN, 1949

ABRONIA GRAY, 1838

***ABRONIA CUYAMA* SP. NOV.**

Zoobank registration: urn:lsid:zoobank.org:pub:8C786137-0AAF-40C5-ABDC-51477AFC4023

Holotype: The holotype *UCMP 54560* is housed in the UCMP and was collected by Gideon T. James and

a party of UCMP palaeontologists in 1957 or 1958. The specimen consists of a partial cranium including the anterior portion of the skull (Figs 2A–F, 3A–E, G–I, 4A), an associated block of mudstone matrix containing a few posterior cranial elements (Figs 2G–I, 3F) and two vials of associated material containing osteoderms in matrix, a probable epipterygoid and unidentified bones.

Etymology: The species is named for the Cuyama Valley Badlands where *UCMP 54560* was collected. 'Cuyama' is derived from the Chumash word *kuyam* (noun) that means 'a place to come together' or 'clam'; the name of the new taxon honours the Chumash people on whose land the fossil was collected.

Diagnosis: Abronia cuyama is a squamate because it has a single premaxilla and pleurodont tooth implantation and an anguimorph because the Meckelian groove is directed ventrally (Estes *et al.*, 1988; Gauthier *et al.*, 1988). The taxon is an anguid because there are rectangular and laterally imbricating osteoderms, a free margin of the intramandibular septum (Gauthier, 1982) and a squamosal that lacks a posteromedial expansion (Bhullar, 2011). The taxon is assigned to Gerrhonotinae because the frontal is fused and lacks suture marks (Klembara *et al.*, 2010; Scarpetta *et al.*, 2021), there is a raised dorsal ossification on each side of the body of the premaxilla (Scarpetta, 2018), and there are no separate palatal processes of the premaxilla (Evans, 2008; Scarpetta *et al.*, 2021). The new taxon shares with *Abronia* excluding species previously placed in *Mesaspis* (Scarpetta *et al.*, 2021) a relatively wide frontal, vermiculate, heavily sculptured osteoderms across the skull, contact of the posterior internasal and prefrontal osteoderms, and the presence of a frontonasal osteoderm (Figs 2A–F, 4A). The osteoderm keels on and anterior to the frontal and the tall osteoderm keels or 'sails' on the posterior cranial osteoderms are autapomorphies of the new taxon (Figs 2H, I, 4A). We performed phylogenetic analyses (see below) to place the new taxon systematically with respect to extant species of *Abronia* and other gerrhonotines.

Description: The specimen is comparable in size to skeletally mature extant gerrhonotines (Fig. 4). Several morphological features previously used to determine skeletal maturity in anguimorphs were not preserved on the fossil (e.g. terminal fusions of the braincase, osteodermal crust on the parietal; Bhullar, 2012), but the robust osteoderms, well-developed osteodermal crust on the frontal and relatively high tooth count (Ledesma *et al.*, 2021) imply a mature individual.

Portions of the alveolar plate, nasal process and incisive process of the premaxilla are preserved (Fig. 3A, B). There are three teeth and several replacement teeth. The nasal process is narrow relative to the width of the alveolar plate and tapers distally almost to a point, and the anterior surface of the process is relatively flat. The alveolar plate lacks discrete palatal processes. The ventral portion of the nasal process is broken, hence the presence of an anterior foramen or an ossified bridge between the nasal process and the alveolar plate cannot be determined. The nasals are present but were difficult to segment from the matrix, and osteoderms are fused to the dorsal surface of the nasals. Some morphological features of the nasals could be observed from the CT slices. Specifically, it was possible to ascertain that the nasals have an anteromedial process that articulates with the nasal process of the premaxilla (xy slice 239; Supporting Information, Fig. S1A) and that the nasals are broadly separated for most of their length, especially anteriorly (xy slice 272; Supporting Information, Fig. S1B) and near their anterior–posterior midpoint (xy slice 448 XY; Supporting Information, Fig. S1C).

Both septomaxillae are present, but only the left septomaxilla was segmented from the surrounding matrix (Fig. 3E). The posterior process is long. The presence of an anterolateral process could not be determined. The maxillae preserve the facial, palatine, premaxillary and orbital processes (Figs 2D, 3C, D). There are six or seven nutrient foramina on the labial surface of both maxillae. There are 18 teeth on the left maxilla, filling all available positions, and on the right maxilla there are 16 teeth and 20 tooth positions. The maxillary lappet projects anterodorsally from the medial surface of the premaxillary process. There is a single foramen (the anterior inferior alveolar foramen) near the anterior edge of the facial process where it meets the premaxillary process. The facial process is inflected medially but does not contact the frontal. The anteroposterior dimension of the facial process is narrow. The palatine process has a slightly rounded subtriangular medial projection. The orbital process is long relative to the facial and premaxillary processes. The posteriormost portion of the left orbital process is broken. Rugose texturing is present on the lateral surface of the maxilla, particularly on the facial process, and some osteoderms are fused to the facial process. The lacrimal is long, extending for nearly half the length of the orbital process of the maxilla, and has rugose sculpturing on its lateral surface. The lacrimal extends both medially and dorsally to enclose, in part, the lacrimal foramen.

The right jugal is present but is missing the posterior portion of the orbital process and dorsal portion of the temporal ramus (Fig. 3H). The temporal ramus has a broad anteroposterior dimension, but the orbital process is more gracile. The orbital process has a ventral lamina that overhangs the dorsal margin
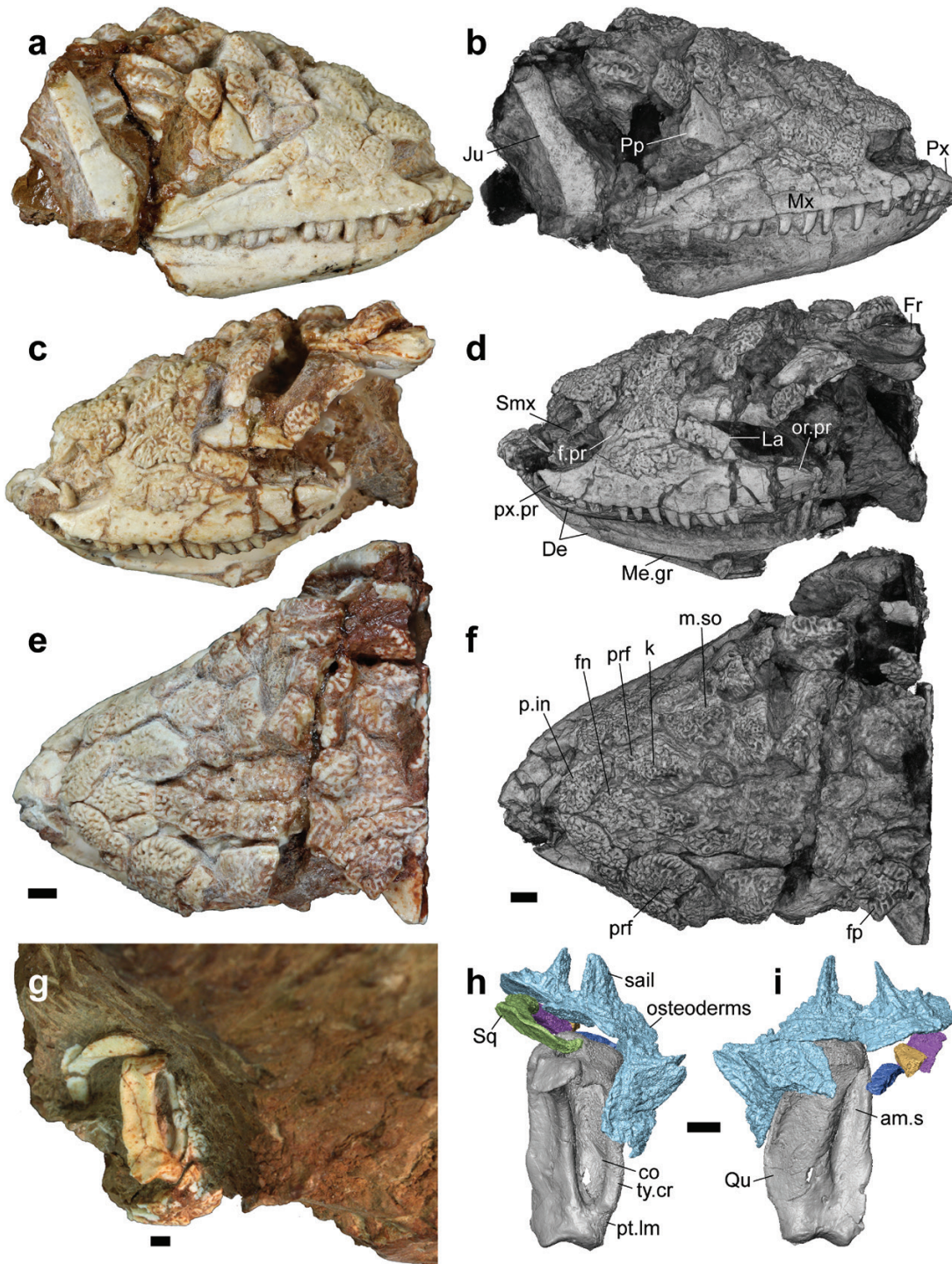
Figure 2. Holotype of *Abronia cuyama* sp. nov. *UCMP 54560*. Images on the left are of the physical specimen and those on the right are digital renderings; B, D and F are volume renderings, whereas H and I are surface renderings. A, B, skull in right lateral view. C, D, skull in left lateral view. E, F, skull in dorsal view. G, quadrate, squamosal and osteoderms from mudstone block in posterior view. H, I, segmented quadrate, squamosal and osteoderms dorsal to the quadrate in posterior and anterior view, respectively. Scale bars: 1 mm. Abbreviations: am.s, anteromedial surface; co, conch; De, dentary; fn, frontonasal; f.pr, facial process; fp, frontoparietal; Fr, frontal; Ju, jugal; k, keel; La, lacrimal; m.so, median supraocular; Me.gr, Meckelian groove; Mx, maxilla; or.pr, orbital process; p.in, posterior internasal; Pp, palpebral; prf, prefrontal; pt.lm, pterygoid lamina; Px, premaxilla; px.pr, premaxillary process; Qu, quadrate; Smx, septomaxilla; Sq, squamosal; ty.cr, tympanic crest.
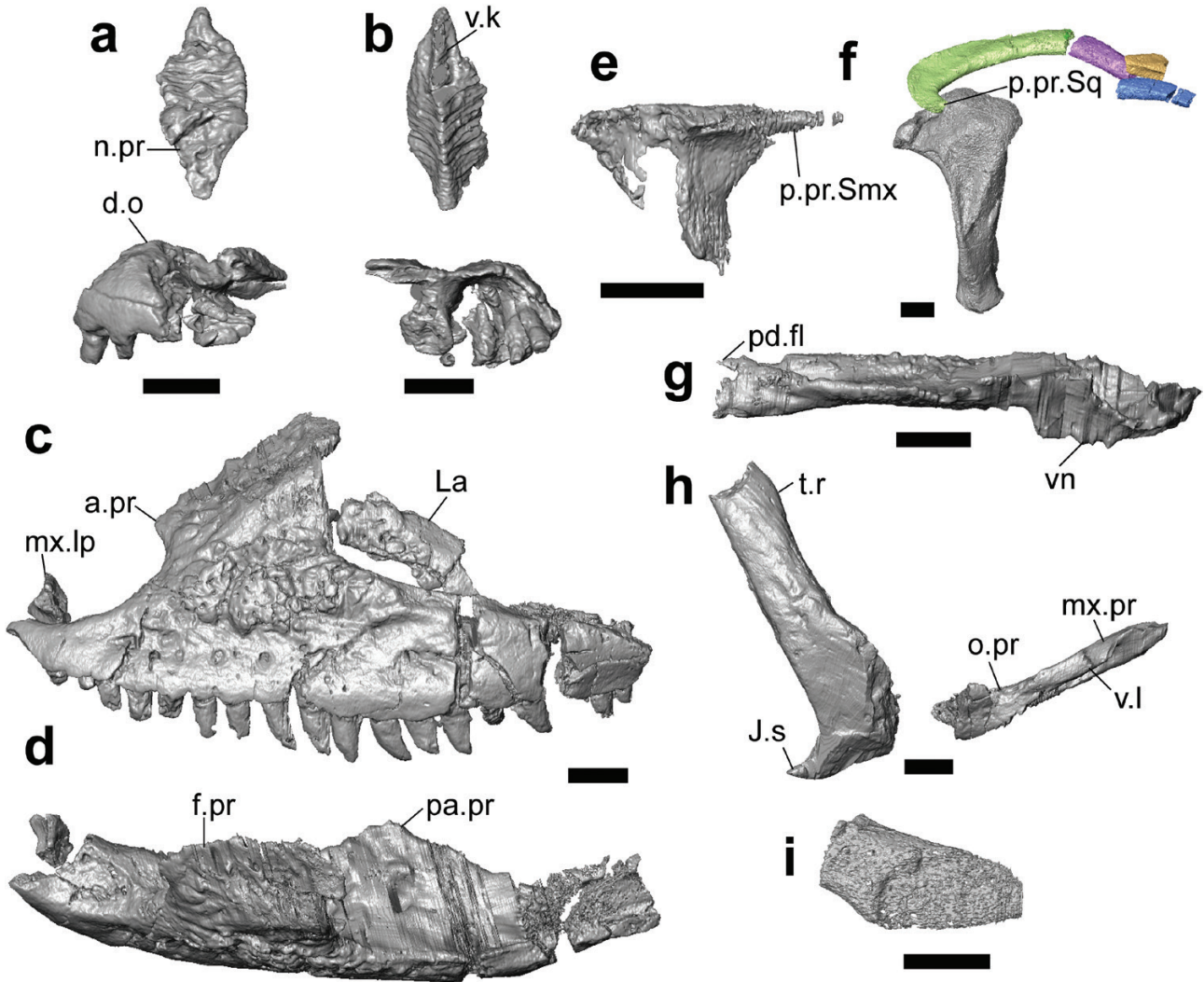
Figure 3. Selected cranial elements of *Abronia cuyama* sp. nov. A, B, premaxilla in anterior and posterior view, respectively. C, D, left maxilla in lateral and dorsal view, respectively. E, left septomaxilla in dorsal view. F, right quadrate and separate pieces of right squamosal in lateral view. G, right vomer in lateral view. H, right jugal in lateral view. I, vomerine process of the left palatine in medial view. Scale bars: 1 mm. Abbreviations: a.pr, anterior process; d.o, dorsal ossification; f.pr, facial process; J.s, jugal spur; La, lacrimal; mx.lp, maxillary lappet; mx.pr, maxillary process; n.pr, nasal process; o.pr, orbital process; pa.pr, palatine process; pd.fl, posterodorsal flange; p.pr.Smx, posterior process of the septomaxilla; p.pr.Sq, posterior process of the squamosal; t.r, temporal ramus; v.k, ventral keel; v.l, ventral lamina; vn, vomeronasal region.

of the orbital process of the maxilla. The jugal spur (quadratojugal process) is large and has a pointed posterior projection. The palpebral is triangular and externally visible.

Both prefrontals are present but were difficult to separate from the matrix. The frontal process is long and projects posterodorsally. The ventral process is short and lacks an anteroventral projection (xy slices 740–750). The prefrontal has a large articulation facet for the facial process of the maxilla. The frontal is complete but broken into an anterior and a posterior piece that are slightly separated from each other (Fig. 2E, F). The frontal is azygous and wide relative to its length. An osteodermal crust covers the dorsal exposure of the frontal, and some osteoderms are fused to the frontal. The anterior process of the frontal is triradiate. The interorbital region is constricted. The facet for the prefrontal on the anterolateral surface of the frontal has small, anterolaterally facing processes at its posterior margin.

Both vomers are present, and the right vomer was segmented (Fig. 3G). There is a dorsally extending posterolateral flange. The anterior (vomeronasal) portion of the bone extends to a lower ventral level than the rest of the element. The foramen for the medial palatine nerve penetrates the right vomer posteriorly
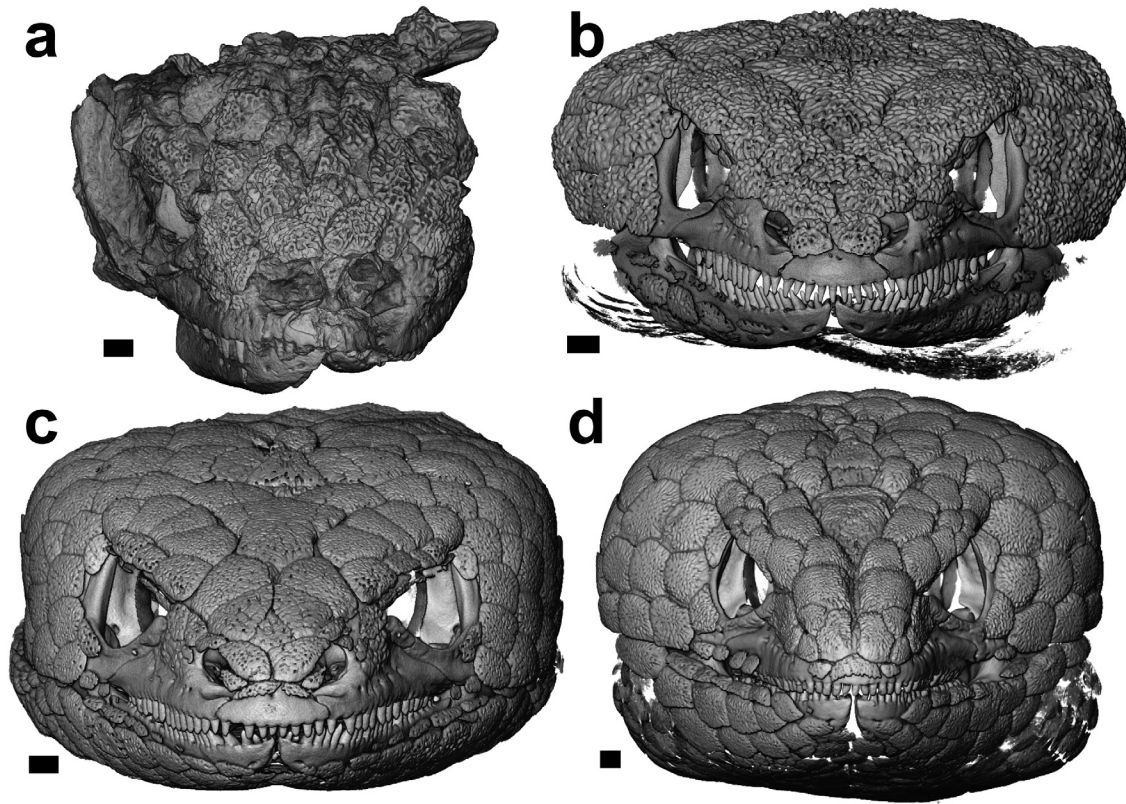
Figure 4. Comparison of *Abronia cuyama* sp. nov. and skulls of extant gerrhonotines, in anterior view. A, *Abronia cuyama* sp. nov. *UCMP 54560*. B, *Abronia graminea UTA 38831*. C, *Elgaria multicarinata* TNHC 35666. D, *Barisia levicollis* MVZ 68783. Scale bars: 1 mm.

and exits anteriorly (xy slices 528–573). The palatines were difficult to segment from the matrix, especially posteriorly. Only the vomerine process was segmented (Fig. 3I), but from the CT slices it was evident that there are no palatine teeth. The vomerine process lacks a posteroventral ridge demarcating the facet for the vomer. There is no anterior flange dorsal to the choana.

The dentaries preserve all but the posterior portion of the bone (Fig. 2B, D). The Meckelian groove is open and is directed ventromedially and ventrally in the anterior and posterior portions of the dentary, respectively. Neither dentary is preserved well enough to ascertain the presence of a surangular process or a posterior groove ventral to the parapet. The free margin of the intramandibular septum is incomplete but present on both sides (for the right dentary, see xy slice 1044; Supporting Information, Fig. S2). There are 22 or 23 tooth positions and 17 teeth on the right dentary and at least ten teeth on the left dentary. Dentition is pleurodont. Crowns on the mesial teeth are unicuspid and sharp, and the crowns on distal teeth are near bicuspid. Teeth are recurved throughout the tooth row of both the dentary and maxilla except for the distalmost teeth. Some of the crowns are missing from the mesial teeth of the right dentary and left

maxilla. The mesial teeth and some of the mid-tooth row teeth of the right maxilla are particularly long, recurved and sharp.

The distal portion of the right squamosal is preserved in the separate mudstone block (Figs 2G–I, 3F). The ventral process curves anterolaterally to articulate with the right quadrate. The element is uniform in width. The right quadrate also is preserved in the block. The quadrate has a narrow mediolateral dimension, with roughly parallel lateral and medial margins. The cephalic condyle is well developed. The mandibular condyle is shaped like a hyperbolic paraboloid and is slightly narrower than the rest of the quadrate. The anteromedial surface of the quadrate is concave, especially dorsally. The pterygoid lamina is shallow, and there is a slightly protruding flange of bone dorsal to it. The column and the tympanic crest are both well developed. The dorsal and ventral portions of the conch are roughly the same width.

The osteoderms are robust and have heavy vermiculate sculpturing (Figs 2A–F, 4A). Osteoderms become more rectangular posteriorly. Many osteoderms have midline keels, including osteoderms anterior to the frontal and the osteodermal crust of the frontal itself. An articulated series of osteoderms (potential temporal

osteoderms) surround the quadrate dorsally, laterally and ventrolaterally (Fig. 2G–I). The osteoderms must have slid ventrally during fossilization, because osteoderms could not occur directly ventral to the quadrate in a live lizard owing to articulation between the quadrate and the mandible. The posterior osteoderms above the quadrate have keels or 'sails' that are more than twice as tall as the osteoderm itself (Fig. 2H, I). The prefrontal, frontonasal and posterior internasal osteoderms are present, and the prefrontals and posterior internasals are in broad contact (Fig. 2E, F). The left prefrontal osteoderm appears to have slipped ventrally from its natural position. Supranasal and anterior internasal osteoderms are not preserved. There is a frontoparietal osteoderm on the left side of the frontal; the osteoderm might have fallen off on the right side. No anteroventral or sublabial osteoderms were preserved.

One of the vials of associated material contains two unidentified bones, which might be weathered osteoderms. The other vial contains two small pieces of mudstone matrix, each with several visible and apparently articulated osteoderms. One of the matrix pieces also contains a tubular bone that is probably an epipterygoid. The osteoderms have the same heavy, vermiculate sculpturing as do those on the skull and in the large mudstone block, and several osteoderms preserve distinct keels.

Comparisons: Comparisons are largely based on the specimens examined by Scarpetta *et al.* (2021). If no specimen number is listed, the comparison accommodates all specimens of a given taxon that we examined for that dataset.

Abronia cuyama has the wide frontal and heavily sculptured vermiculate-textured osteoderms that are characteristic of *Abronia*, excluding, among examined specimens, *Abronia monticola* Cope, 1878, *Abronia moreletti* Bocourt, 1872 and *Abronia gadovii* Boulenger, 1913 (i.e. species previously placed in *Mesaspis*). The anterodorsal osteoderms of *Barisia imbricata* Wiegmann, 1828 and *Barisia ciliaris* Smith, 1942 are also heavily sculptured. The facial process of the maxilla is narrow in *Abronia campbelli* Brodie & Savage, 1993, *Abronia lythrochila* Smith & Alvarez del Toro, 1963, *A. moreletti*, *A. monticola*, *A. gadovii*, *G. parvus* SRSU 5538 and some observed specimens of *Elgaria panamintina* Stebbins, 1958 and *Elgaria velazquezi* Grismer & Hollingsworth, 2001 (MVZ 191076 and SDNHM 68678, respectively). Several species of *Abronia* (e.g. *Abronia graminea* Cope, 1864, *A. ornelasi* and *A. gadovii*), *Barisia* (*Barisia levicollis* Stejneger, 1890, *B. ciliaris* and *B. imbricata*) and *D. lugoi* have nasals that are separated near their longitudinal midpoint. The quadrate conch is largely uniform in width in *A. campbelli*, *A. lythrochila*,

A. gadovii and several specimens of *Barisia* (e.g. *B. ciliaris* FMNH 30707). The vomeronasal region of the vomer is ventrally displaced in *A. campbelli*, *A. lythrochila*, *A. graminea*, *A. ornelasi* and *A. gadovii*. The vomerine process of the palatine lacks a ventral ridge in most *Abronia*, but the ridge is present in *Abronia mixteca* Bogert & Porter, 1967 and *A. gadovii*. Species previously referred to *Mesaspis* and *Abronia taeniata* Wiegmann, 1828 (TCWC 30660) have an osteoderm overlying the frontoparietal scute. Examined specimens of *Barisia* and *Abronia*, excluding *A. ornelasi* and species previously placed in *Mesaspis*, display contact of the posterior internasal and prefrontal osteoderms. *Abronia cuyama* has a frontonasal osteoderm, which is absent in *Barisia* (Fig. 4D), and has a flat anterior surface of the nasal process of the premaxilla, unlike *Barisia*.

The extinct gerrhonotines *P. ricardensis* and *G. mungerorum* were previously suggested to be part of or closely related to *Abronia* based primarily on the presence of heavily sculptured osteoderms and relatively long, fang-like teeth (Good, 1988a), but neither was ever formally placed in *Abronia*. *Paragerrhonotus ricardensis* was described from a partial skull (Estes, 1963). Phylogenetic studies that included *P. ricardensis* placed the taxon in a polytomy with *Gerrhonotus*, *Barisia* and *Abronia* or as a stem gerrhonotine (Conrad & Norell, 2008; Norell *et al.*, 2008). Based on examination of the holotype and with reference to the diagnostic characters listed by Estes (1963), *P. ricardensis* and *A. cuyama* share heavily sculptured osteoderms (although the texture is less vermiculate in *Paragerrhonotus*, similar to *Barisia*), a large jugal spur, and sharp, recurved mesial teeth on the maxilla. A large jugal spur and sharp and recurved maxillary teeth are present in many gerrhonotines (Gauthier, 1982; Ledesma *et al.*, 2021; Scarpetta *et al.*, 2021), and neither was used here as a phylogenetic character. *Paragerrhonotus ricardensis* differs from *A. cuyama* in possessing an elongate frontal, in lacking osteoderm keels, in lacking a ventral lamina of the orbital process of the jugal, in possessing a distinctive arrangement of small osteoderms on the posterior portion of the frontal (not adapted as a phylogenetic character) and in possessing a premaxillary nasal process with a concave dorsal surface. *Abronia cuyama* and *P. ricardensis* do not share any unique synapomorphies or apomorphic character state combinations.

We also note that *P. ricardensis* has a single row of four pterygoid teeth, as originally stated by Estes (1963) and *contra* Good (1988a). The loss of pterygoid teeth is another feature mentioned by Good (1988a) to suggest a close relationship between *P. ricardensis* and *Abronia*. The loss of pterygoid teeth was interpreted by several authors as a derived feature of *Abronia*

and *Barisia* (Good, 1987; Scarpetta *et al.*, 2021). A few examined specimens of *Abronia* and *Barisia* have one to three irregularly arranged pterygoid teeth (e.g. *A. campbelli* UTA 95952; *B. ciliaris* FMNH 30707).

Gerrhonotus mungerorum was described based on a single, isolated frontal (Wilson, 1968). Additional fossils, including partial dentaries, maxillae and a parietal, were later attributed to the taxon from the type locality and other localities (e.g. Holman, 1973, 1975), but those identifications were either explicitly tentative or based on features not unique to *G. mungerorum* with respect to other gerrhonotines. *Gerrhonotus mungerorum* requires further study, especially the tentatively referred fossils, and a systematic assessment of the species would benefit from the procurement of additional fossils from the type locality. We have not examined the holotype or attributed specimens of *G. mungerorum* in person; therefore, based on the description of the holotype and descriptions of referred fossils, *G. mungerorum* and *A. cuyama* share a heavily sculptured frontal, sharp and recurved teeth, and the presence of near bicuspid crowns on the distal teeth. Sharp and recurved teeth and near bicuspid distal crowns are common to many gerrhonotines (Scarpetta *et al.*, 2021), and the former was not used as a phylogenetic character. *Gerrhonotus mungerorum* differs from *A. cuyama* in having an elongate frontal and in lacking keels on the frontal osteoderm crust.

Cranial osteoderm keels are present in *Elgaria multicarinata* Blainville, 1835 and *Elgaria nana* Fitch, 1934, although neither of those species has osteoderm keels anterior to the frontal or on the frontal (Ledesma *et al.*, 2021; Scarpetta *et al.*, 2021). Among other squamates, nuchal osteoderm sails were observed on *Cordylus namakuiyus* Stanley, Ceríaco, Bandeira, Valerio, Bates & Branch, 2016 and *Cordylus angolensis* Bocage, 1895 (CAS 254912 and AMNH 47333, respectively). Among other anguimorphs, postcranial osteoderm keels were observed in *Shinisaurus crocodilurus* Ahl, 1930 (UF 45615 and FMNH 215541), and keels are present on some cranial osteoderms and the frontal osteodermal crust in some *Xenosaurus* (e.g. *Xenosaurus grandis* Gray, 1856; FMNH 123702).

PHYLOGENETIC ANALYSES

We performed unconstrained and constrained specimen-based analyses using Bayesian inference and parsimony. In the unconstrained and partially constrained analyses, the *Mesaspis* and *Abronia* morphotypes were monophyletic and sister taxa, as in previous morphological analyses (Good, 1987, 1988b; Campbell & Frost, 1993; Scarpetta *et al.*, 2021). In the fully constrained Bayesian analyses, *A. cuyama* was inferred as the sister taxon of the subgenus *Auriculabronia* Campbell & Frost, 1993 (here represented by *A. campbelli* and *A. lythrochila*) with high posterior probability (Fig. 5B and Supporting Information, Fig. S3); that clade is found east of the Isthmus of Tehuantepec in the modern biota (Campbell & Frost, 1993; Gutiérrez-Rodríguez *et al.*, 2021). In the unconstrained (Supporting Information, Fig. S5) and partially constrained (Fig. 5A and Supporting Information, Fig. S4) Bayesian analyses, that relationship was inferred but not strongly supported. In
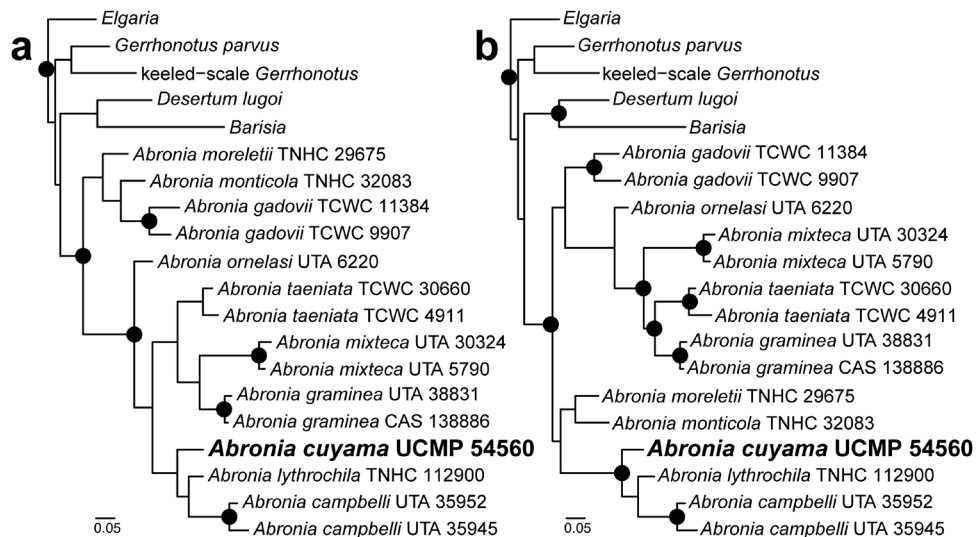
Figure 5. Phylogenetic position of *Abronia cuyama* sp. nov. among alligator lizards in Bayesian inference analyses. A, partially constrained tree. B, fully constrained tree. Outgroups are removed for clarity, and other gerrhonotine genera or species are condensed to single terminals. Black circles indicate nodes with posterior probability > 0.95.

all strict consensus trees from the parsimony analyses. *A. cuyama* was in a polytomy with *A. campbelli* and *A. lythrochila* (Supporting Information, Figs S6–S8). The position of *A. cuyama* within crown *Abronia* is supported regardless of topology or the analytical method used here. However, a close relationship with *Auriculabronia* should be considered tentative at best, given the low support values in the partially constrained and unconstrained trees from the Bayesian analyses.

DISCUSSION

Abronia cuyama is the first definitive fossil and only described extinct species of *Abronia* and is a significant discovery in terms of both biogeography and morphology. The dorsal cranial osteoderms are robust and heavily sculptured, like many modern species of *Abronia*, but there is no precedent among examined gerrhonotines for the striking posterior osteoderm sails or the keels on the anterior cranial osteoderms. Osteoderm sails should be added as a character to the matrix published by Scarpetta *et al.* (2021) should more specimens of *A. cuyama* or other gerrhonotine taxa with osteoderm sails be discovered.

The discovery of *A. cuyama* elicits a different biogeographical history of *Abronia* from that which could be inferred from the distribution and phylogeny of the extant species alone. The possibility and implications of extralimital Neogene occurrences of *Abronia* have been discussed previously with respect to *G. mungerorum* in Kansas and *P. ricardensis* in California (Good, 1985, 1988a). Although *G. mungerorum* and *P. ricardensis* provided the first potential evidence that *Abronia* might once have inhabited areas north of Mexico, neither extinct taxon was ever formally placed in *Abronia*, and the taxonomic status of those two extinct species is still uncertain. Thus, *A. cuyama* provides the first demonstrable record of *Abronia* in what is now the USA. Extant *Abronia* inhabit many mountain ranges in Mesoamerica but are conspicuously absent from the SMO (Fig. 1), although most orogenic activity occurred there before the middle Miocene (Ferrari *et al.*, 2007). *Barisia*, another montane alligator lizard and the sister group of *Abronia* (Zheng & Wiens, 2016; García-Vázquez *et al.*, 2018; Blair *et al.*, 2022), is widely distributed in the SMO in the modern biota, and the two clades are sympatric in other montane regions in central and southern Mexico (Bryson & Riddle, 2012; Gutiérrez-Rodríguez *et al.*, 2021). The presence of *A. cuyama* on the Pacific coast of California might imply ancestral occupation of the SMO by *Abronia* and the most recent common ancestor of *Abronia* and *Barisia*. The SMO probably contained suitable habitat for *Abronia* from the Miocene to the present day (i.e.

temperate to subtropical deciduous and evergreen forest; Axelrod, 1979; Pound *et al.*, 2012; Rodríguez-Veiga *et al.*, 2016), assuming conserved ecology of *Abronia* throughout the history of the clade. Moreover, the palaeobotanical record indicates the presence of warm-temperate evergreen broadleaf and mixed forest in south-eastern Mexico, northern Mexico and the western USA during the middle Miocene (Pound *et al.*, 2012). Rifting in the Gulf of California did not begin until the late Miocene (Blakey & Ranney, 2018, Ferrari *et al.*, 2018), and the Sonoran Desert did not attain its modern aridity and plant communities until the late Pliocene or Pleistocene (Axelrod, 1979), hence dispersal of montane taxa between the SMO and the mountains of coastal California would not have been as improbable during the early or middle Miocene as it would be currently.

Ultimately, the Caliente Formation is so far outside the modern range of *Abronia* that more fossils, in addition to expanded genomic and morphological datasets, will be necessary to investigate the biogeography of *Abronia* and to determine when and why *Abronia* was extirpated from areas north and west of its present distribution. Although the fossil record of lizards in the continental USA indicates a general shift in composition from mostly megathermal taxa early in the Cenozoic (e.g. Smith & Gauthier, 2013) to more temperate taxa during the Miocene (e.g. Scarpetta, 2021), there are at least a few other records indicating the persistence of extant tropical taxa. Unsurprisingly, those records, consisting of several fossil anoles and basilisk lizards, are in peninsular Florida (Chovanec, 2014). The collection and description of additional fossil lizards might reveal additional instances of longer-term persistence of megathermal taxa and/or post-Palaeogene migration of lizards from tropical or subtropical Mexico into temperate latitudes of North America.

The documented record of fossil mammals from the Miocene of Mexico adds some information to the biogeographical understanding of *A. cuyama*. Camel and lagomorph genera of late early and middle Miocene age (Ferrusquía-Villafranca, 2003; Montellano-Ballesteros & Jiménez-Hidalgo, 2006) are shared between the SMO (Tubutama and Yécora) and the mammal faunas of the USA broadly, including those of the western portion of the country. Gomphotheres and rhinos are shared between the middle Miocene of Chiapas (Ixtapa) and the USA, and merychippine, hipparionine and equine horses known from Oaxaca (Nejapa) during the middle Miocene were hypothesized to potentially represent southward migration to subtropical Mexico from temperate latitudes (Ferrusquía-Villafranca, 2003). Although there are few Clarendonian faunas in Mexico, migration between the temperate and subtropical zones seems to have

occurred among large-bodied mammals. Study of less vagile, smaller-bodied vertebrates, such as mammals and squamates, could help to provide further information on the biogeography of *A. cuyama* and the potential for migration in *Abronia* generally.

Interpretation of *A. cuyama* as a member of crown *Abronia* is supported by all phylogenetic analyses presented here; the fossil was not placed as the sister taxon of *Abronia* or elsewhere on the tree in any analysis that we performed. The age of the fossil (12.5–11.0 Mya), which was deposited ~12 Mya after the putative appearance of crown *Abronia* (Zheng & Wiens, 2016), provides supplemental support for that conclusion. Given the number of shared characters between *A. cuyama* and members of crown *Abronia* (particularly the arboreal, *Abronia* morphotype species), we think it is highly unlikely that *A. cuyama* would cluster with one of the other gerrhonotine genera in any future analysis. *Abronia cuyama* shares several character states with species of *Auriculabronia* (represented here by *A. campbelli* and *A. lythrochila*) and was consistently placed with that subgenus in phylogenetic analyses. However, none of those characters is exclusive to examined species of *Auriculabronia* (see Comparisons), and that relationship was not always inferred with high support. Additionally, *A. cuyama* and *A. taeniata* are the only sampled *Abronia* morphotype species that have a frontoparietal osteoderm. Nine extant species of *Abronia* were sampled here, representing six of 11 subclades of *Abronia* (Campbell & Frost, 1993; Gutiérrez-Rodríguez *et al.*, 2021; Scarpetta *et al.*, 2021), but 32 recognized species were not sampled (García-Vázquez *et al.*, 2022); augmented sampling of extant species might refine our understanding of the phylogenetic relationships of *A. cuyama* with the extant species of *Abronia*. Thus, we emphasize that any attribution of *A. cuyama* to *Auriculabronia* (or the eastern clade more broadly) is tentative. We suggest that *UCMP 54560* might be used most conservatively as a node calibration to anchor the minimum age of the divergence between *Abronia* and *Barisia*.

Although neither *G. mungerorum* or *P. ricardensis* was included in our phylogenetic analyses (because the holotype and attributed specimens of *G. mungerorum* require further study, and *P. ricardensis* will be the subject of a separate project), we provide several morphological differences between those taxa and *A. cuyama*. These differences include features mentioned in the original descriptions of *G. mungerorum* and *P. ricardensis* and in characters used in the phylogenetic analyses of the present study. Differences in the phylogenetic character states, in particular, demonstrate that *A. cuyama* is distinct from and should not be assigned to either previously described extinct species.

The ecological history of *Abronia* is not inherently modified by the discovery of *A. cuyama*. Extant species from both the eastern and western clades are found in seasonally dry pine-oak forest (e.g. *A. lythrochila* and *A. mixteca*, respectively; Campbell & Frost, 1993); therefore, the palaeoenvironment of the Caliente Formation was not necessarily outside the known ecological tolerances of *Abronia*. Sediments from the Caliente Formation are fluvial in origin, and the formation was bounded by mountains when it was deposited, raising the possibility that *UCMP 54560* was transported from a higher elevation to the location where it was preserved. Interpretation of microfossil accretions as disarticulated owl pellets further the potential for transport of the fossil before deposition. Although owls display high roost fidelity, individual species may consume prey from heterogeneous ecosystems; therefore, it is possible that the fossil had been transported from a nearby area with a different environment from that of the Caliente Formation (Saavedra & Simonetti, 1998; Terry, 2004). On the contrary, James (1963) suggested that a diurnal ground owl could be responsible for the hypothesized pellets, in which case *UCMP 54560* would probably not have been transported from elsewhere.

Abronia cuyama exemplifies the importance of palaeontological data for biogeography. There are many fossil lizards that defy biogeographical expectations based on the modern biota, such as extinct iguanian lizards that were found across oceans and in different hemispheres from modern representatives (Smith, 2009; Smith & Gauthier, 2013; Simões *et al.*, 2015). Inclusion of extralimital fossil occurrences improves taxon-specific biogeographical analyses (Tavares *et al.*, 2018), and by extension, integrative analyses that infer the assembly of ecosystems through time and space should be improved by inclusion of palaeontological data. The discovery of *A. cuyama* confirms the presence of *Abronia* in the Neogene of the USA, indicates that the faunal assembly of coastal California has changed substantively through time and hints that, broadly, montane taxa of modern Mesoamerica were more geographically diffuse during the Neogene. Hopefully, this discovery will stimulate investigations of biogeographical links between the mountains of southern Mexico, the SMO and the mountains of the south-western USA and augment future biogeographical studies of montane Mesoamerica (e.g. Ornelas *et al.*, 2013).

ACKNOWLEDGEMENTS

ElShafie provided helpful early discussions on the affinity of the fossil. We thank Pat Holroyd and UCMP for access to the fossil, and the museum collections, curators and collections of FMNH, MVZ, TNHC, SDNHM, TCWC, UF and UTA for access to other specimens. S.G.S. thanks Chris Bell, Dan Breecker, David Cannatella, Travis LaDuc, Tim Rowe and Krister Smith for feedback on the manuscript. We thank two anonymous reviewers for providing detailed and constructive suggestions that greatly improved the manuscript.

FUNDING

DATA AVAILABILITY

All CT data from extant specimens are available at MorphoSource.org (for all media links, see Scarpetta *et al*. 2021). The CT data for *UCMP 54560* are deposited at MorphoSource.org (project https://www.morphosource.org/projects/000393302, media 000429682 and 000429646). Supplemental figures and tables are in the Supporting Information (Supplemental File 1), and the R script for the phylogenetic character binning analyses is in the Supporting Information (Supplemental File 2). The phylogenetic matrix and program commands are deposited as Supporting Information (Supplemental Files 3 and 4 for the Bayesian and parsimony analyses, respectively).

REFERENCES

Axelrod DI. 1940. The Mint Canyon flora of southern California: a preliminary statement. *American Journal of Science* **238:** 577–585.

Axelrod DI. 1979. Age and origin of Sonoran Desert vegetation. *Occasional Papers of the California Academy of Science* **132:** 1–74.

Barnosky AD, **Holmes M**, **Kirchholtes R**, **Lindsey E**, **Maguire KC**, **Poust AW**, **Stegner MA**, **Sunseri J**, **Swartz B**, **Swift J**, **Villavicencio NA**, **Wogan GO. 2014.** Prelude to the Anthropocene: two new North American land mammal ages (NALMAs). *The Anthropocene Review* **1:** 225–242.

Bhullar B-AS. 2011. The power and utility of morphological characters in systematics: a fully resolved phylogeny of *Xenosaurus* and its fossil relatives (Squamata: Anguimorpha). *Bulletin of the Museum of Comparative Zoology* **160:** 65–181.

Bhullar B-AS. 2012. A phylogenetic approach to ontogeny and heterochrony in the fossil record: cranial evolution and development in anguimorphan lizards (Reptilia: Squamata). *Journal of Experimental Zoology. Part B. Molecular and Developmental Evolution* **318:** 521–530.

Blair C, **Bryson RW Jr**, **García-Vázquez UO**, **Nieto-Montes de Oca A**, **Lazcano D**, **McCormack JE**, **Klicka J. 2021.** Phylogenomics of alligator lizards elucidate diversification patterns across the Mexican Transition Zone and support the recognition of a new genus. *Biological Journal of the Linnean Society* **135:** 25–39.

Blakey RC, **Ranney WD. 2018.** *Ancient landscapes of western North America: a history with paleogeographic maps*. Cham: Springer Nature.

Bryson RW Jr, **Riddle BR. 2012.** Tracing the origins of widespread highland species: a case of Neogene diversification across the Mexican sierras in an endemic lizard. *Biological Journal of the Linnean Society* **105:** 382–394.

Campbell JA, **Frost DR. 1993.** Anguid lizards of the genus *Abronia*: revisionary notes, descriptions of four new species, a phylogenetic analysis, and key. *Bulletin of the American Museum of Natural History* **216:** 1–121.

Chovanec K. 2014. *Non-anguimorph lizards of the Late Oligocene and Early Miocene of Florida and implications for the reorganization of the North American herpetofauna*. Unpublished MSc. Thesis, East Tennessee State University.

Clause AG, **Luna-Reyes R**, **Nieto-Montes de Oca A. 2020.** A new species of *Abronia* (Squamata: Anguidae) from a protected area in Chiapas, Mexico. *Herpetologica* **76:** 330–343.

Conrad JL, **Norell MA. 2008.** The braincases of two glyptosaurines (Anguidae, Squamata) and anguid phylogeny. *American Museum Novitates* **3613:** 1–24.

Ehlert KW. 2003. Tectonic significance of the middle Miocene Mint Canyon and Caliente Formations, southern California. In: Crowell JC, ed. *Evolution of Ridge Basin, southern California: an interplay of sedimentation and tectonics*. Boulder: Geological Society of America, 113–130.

Estes R. 1963. A new gerrhonotine lizard from the Pliocene of California. *Copeia* **1963:** 676–680.

Estes R. 1983. *Encyclopedia of paleoherpetology, Sauria terrestria, Amphisbaenia*. Stuttgart: Gustav Fisher.

Estes R, **De Queiroz K**, **Gauthier JA. 1988.** Phylogenetic relationships within Squamata. In: Estes R, Pregill GK, eds. *Phylogenetic relationships of the lizard families: essays commemorating Charles L. Camp*. Stanford: Stanford University Press, 119–281.

Evans SE. 2008. The skull of lizards and tuatara. In: Gans C, Gaunt AS, Adler K, eds. *Biology of the Reptilia, Vol. 20, morphology H: the skull of Lepidosauria*. Ithaca: Society for the Study of Amphibians and Reptiles, 1–347.

Evernden JF, **Savage DE**, **Curtis GH**, **James GT. 1964.** Potassium-argon dates and the Cenozoic mammalian chronology of North America. *American Journal of Science* **262:** 145–198.

Ferrari L, **Orozco-Esquivel T**, **Bryan SE**, **López-Martínez M**, **Silva-Fragoso A. 2018.** Cenozoic magmatism and extension in western Mexico: linking the Sierra Madre Occidental silicic large igneous province and the Comondú

Group with the Gulf of California rift. *Earth-Science Reviews* **183:** 115–152.

Ferrari L, **Valencia-Moreno M**, **Bryan S. 2007.** Magmatism and tectonics of the Sierra Madre Occidental and its relation with the evolution of the western margin of North America. In: Alaniz-Álvarez SA, Nieto-Samaniego ÁF, eds. *Geology of México: celebrating the centenary of the Geological Society of México*. Boulder: Geological Society of America, 1–39.

Ferrusquía-Villafranca I. 2003. Mexico's middle Miocene mammalian assemblages: an overview. *Bulletin of the American Museum of Natural History* **279:** 321–347.

García-Vázquez UO, **Clause AG**, **Gutiérrez-Rodríguez J**, **Cazares-Hernández E**, **de la Torre Loranca MA. 2022.** A new species of *Abronia* (Squamata: Anguidae) from the Sierra de Zongolica of Veracruz, Mexico. *Ichthyology & Herpetology* **110:** 33–49.

García-Vázquez UO, **Nieto-Montes de Oca A**, **Bryson RW Jr**, **Shmidt-Ballardo W**, **Pávon-Vázquez CJ. 2018.** Molecular systematics and historical biogeography of the genus *Gerrhonotus* (Squamata: Anguidae). *Journal of Biogeography* **45:** 1640–1652.

Gauthier JA. 1982. Fossil xenosaurid and anguid lizards from the early Eocene Wasatch Formation, southeast Wyoming, and a revision of the Anguioidea. *Contributions to Geology, University of Wyoming* **21:** 7–54.

Gauthier JA, **Estes R**, **De Queiroz K. 1988.** Phylogenetic relationships within Squamata. In: Estes R, Pregill GK, eds. *Phylogenetic relationships of the lizard families: essays commemorating Charles L. Camp*. Stanford: Stanford University Press, 15–98.

GBIF.org. **2021.** *GBIF occurrence download*. Available at: https://doi.org/10.15468/dl.e4q2cr (generated 4 February 2021).

Good DA. 1985. *Studies of interspecific and intraspecific variation in the alligator lizards (Lacertilia: Anguidae: Gerrhonotinae)*. Unpublished PhD Thesis, University of California, Berkeley.

Good DA. 1987. A phylogenetic analysis of cranial osteology in the gerrhonotine lizards. *Journal of Herpetology* **21:** 285–297.

Good DA. 1988a. The phylogenetic position of fossils assigned to the Gerrhonotinae (Squamata: Anguidae). *Journal of Vertebrate Paleontology* **8:** 188–195.

Good DA. 1988b. Phylogenetic relationships among Gerrhonotinae lizards: an analysis of external morphology. *University of California Publications in Zoology* **121:** 1–139.

Google Earth Pro. **2021.** *34°48′51.00″N, 119°17′6.75″W*. Available at: http://www.earth.google.com (accessed 14 March 2021).

Gutiérrez-Rodríguez J, **Zaldívar-Riverón A**, **Solano-Zavaleta I**, **Campbell JA**, **Meza-Lázaro RN**, **Flores-Villela O**, **Nieto-Montes de Oca A. 2021.** Phylogenomics of the Mesoamerican alligator-lizard genera *Abronia* and *Mesaspis* (Anguidae: Gerrhonotinae) reveals multiple independent clades of arboreal and terrestrial species. *Molecular Phylogenetics and Evolution* **154:** 106973.

Holman JA. 1973. Reptiles of the Egelhoff herpetofauna (Upper Miocene) of Nebraska. *Contributions from the Museum of Paleontology University of Michigan* **24:** 125–134.

Holman JA. 1975. Herpetofauna of the WaKeeney local fauna (Lower Pliocene: Clarendonian) of Trego County, Kansas. *University of Michigan Papers on Paleontology* **12:** 49–66.

Hoyt JF, **Coffey KT**, **Ingersoll RV**, **Jacobson CE. 2018.** Paleogeographic and paleotectonic setting of the Middle Miocene Mint Canyon and Caliente Formations, southern California: an integrated provenance study. In: Ingersoll V. Lawton TF, Graham SA, eds. *Tectonics, sedimentary basins, and provenance: a celebration of William R. Dickinson's career: Geological Society of America Special Paper 540*. Boulder: Geological Society of America, 463–480.

IUCN. **2022.** *IUCN red list of threatened species*. *Version 2021-3*. Available at: www.iucnredlist.org (accessed 15 March 2021).

James GT. 1963. Paleontology and nonmarine stratigraphy of the Cuyama Valley Badlands, California. Part I. Geology, faunal interpretations, and systematic descriptions of Chiroptera, Insectivora, and Rodentia. *University of California Publications in Geological Sciences* **45:** iv + 171.

Jennings CW. (with modifications by Gutierrez C, Bryant W, Saucedo G, Wills C). **2010.** *Geologic Map of California: California Geological Survey Geologic Data Map 2, scale 1:750,000*. Available at: https://gis.data.ca.gov/datasets/95 4c14d3baf64f27849c46b219113d2d (accessed 23 February 2021).

Klembara J, **Böhme M**, **Rummel M. 2010.** Revision of the anguine lizard *Pseudopus laurillardi* (Squamata, Anguidae) from the Miocene of Europe, with comments on paleoecology. *Journal of Paleontology* **84:** 159–196.

Leavitt DH, **Marion AB**, **Hollingsworth BD**, **Reeder TW. 2017.** Multilocus phylogeny of alligator lizards (*Elgaria*, Anguidae): testing mtDNA introgression as the source of discordant molecular phylogenetic hypotheses. *Molecular Phylogenetics and Evolution* **110:** 104–121.

Ledesma DT, **Scarpetta SG**, **Bell CJ. 2021.** Variation in the skulls of *Elgaria* and *Gerrhonotus* (Anguidae, Gerrhonotinae) and implications for phylogenetics and fossil identification. *PeerJ* **9:** e11602.

Montellano-Ballesteros M, **Jiménez-Hidalgo E. 2006.** Mexican fossil mammals, who, where and when? In: Vega FJ, Torrey GN, Perrilliat MC, Montellano M, Cevallos S, Quiroz S, eds. *Studies on Mexican paleontology*. The Hague: Springer, 249–273.

Norell MA. 1989. Late Cenozoic lizards of the Anza Borrego Desert, California. *Contributions in Science, Natural History Museum of Los Angeles County* **414:** 1–31.

Norell MA, **Gao K**, **Conrad J. 2008.** A new platynotan lizard (Diapsida: Squamata) from the Late Cretaceous Gobi Desert. *American Museum Novitates* **3605:** 1–22.

Ornelas JF, **Sosa V**, **Soltis DE**, **Daza JM**, **González C**, **Soltis PS**, **Gutiérrez-Rodríguez C**, **de los Monteros AE**, **Castoe TA**, **Bell C**, **Ruiz-Sanchez E. 2013.** Comparative phylogeographic analyses illustrate the complex evolutionary history of threatened cloud forests of northern Mesoamerica. *PLoS One* **8:** e56283.

Pound MJ, **Haywood AM**, **Salzmann U**, **Riding JB. 2012.** Global vegetation dynamics and latitudinal temperature

gradients during the Mid to Late Miocene (15.97–5.33 Ma). *Earth-Science Reviews* **112:** 1–22.

Prothero DR, **Kelly TS**, **McCardel KJ**, **Wilson EL. 2008.** Magnetostratigraphy, biostratigraphy, and tectonic rotation of the Miocene Caliente Formation, Ventura County, California. *New Mexico Museum of Natural History and Science Bulletin* **44:** 255–272.

Raffi I, **Wade BS**, **Pälike H**, **Beu AG**, **Cooper R**, **Crundwell MP**, **Krijgsman W**, **Moore T**, **Raine I**, **Sardella R**, **Vernyhorova YV. 2020**. In: Gradstein FM, Ogg JG, Schmitz MD, Ogg GM, eds. *The geologic time scale 2020*. Amsterdam: Elsevier, 1141–1215.

Rambaut A, **Drummond AJ**, **Xie D**, **Baele G**, **Suchard MA. 2018.** Posterior summarization in Bayesian phylogenetics using Tracer 1.7. *Systematic Biology* **67:** 901–904.

Rodríguez-Veiga P, **Saatchi S**, **Tansey K**, **Balzter H. 2016.** Magnitude, spatial distribution and uncertainty of forest biomass stocks in Mexico. *Remote Sensing of Environment* **183:** 265–281.

Ronquist F, **Teslenko M**, **Van der Mark P**, **Ayres DL**, **Darling A**, **Höhna S**, **Larget B**, **Liu L**, **Suchard MA**, **Huelsenbeck JP. 2012.** MrBayes 3.2: efficient Bayesian phylogenetic inference and model choice across a large model space. *Systematic Biology* **61:** 539–542.

Saavedra B, **Simonetti JA. 1998.** Small mammal taphonomy: intraspecific bone assemblage comparison between South and North American barn owl, *Tyto alba*, populations. *Journal of Archaeological Science: Reports* **25:** 165–170.

Scarpetta S. 2018. The earliest known occurrence of *Elgaria* (Squamata: Anguidae) and a minimum age for crown Gerrhonotinae: fossils from the Split Rock Formation, Wyoming, USA. *Palaeontologia Electronica* **21.1.1FC:** 1–9.

Scarpetta SG. 2021. Iguanian lizards from the Split Rock Formation, Wyoming: exploring the modernization of the North American lizard fauna. *Journal of Systematic Palaeontology* **19:** 2211–2251.

Scarpetta SG, **Ledesma DT**, **Bell CJ. 2021.** A new extinct species of alligator lizard (Squamata: *Elgaria*) and an expanded perspective on the osteology and phylogeny of Gerrhonotinae. *BMC Ecology and Evolution* **21:** 1–58.

Simões TR, **Wilner E**, **Caldwell MW**, **Weinschütz LC**, **Kellner AWA. 2015.** A stem acrodontan lizard in the Cretaceous of Brazil revises early lizard evolution in Gondwana. *Nature Communications* **6:** 8149.

Smith KT. 2009. A new lizard assemblage from the earliest Eocene (Zone WA0) of the Bighorn Basin, Wyoming, USA: biogeography during the warmest interval of the Cenozoic. *Journal of Systematic Palaeontology* **7:** 299–358.

Smith KT, **Gauthier JA. 2013.** Early Eocene lizards of the Wasatch Formation near Bitter Creek, Wyoming: diversity and paleoenvironment during an interval of global warming. *Bulletin of the Peabody Museum of Natural History* **54:** 135–230.

Solano-Zavaleta I, **Nieto-Montes de Oca A. 2018.** Species limits in the Morelet's alligator lizard (Anguidae: Gerrhonotinae). *Molecular Phylogenetics and Evolution* **120:** 16–27.

Swofford, D. L. 2003. *PAUP*: phylogenetic analysis using parsimony (*and other methods), Version 4*. Sunderland: Sinauer Associates.

Tavares VC, **Warsi OM**, **Balseiro F**, **Mancina CA**, **Dávalos LM. 2018.** Out of the Antilles: fossil phylogenies support reverse colonization of bats to South America. *Journal of Biogeography* **45:** 859–873.

Tedford RH, **Alrbright LBA**, **Barnosky AD**, **Ferrusquia-Villafranca I**, **Hunt RMJ**, **Storer JE**, **Swisher CC**, **Voorhies MR**, **Webb SD**, **Whistler DP. 2004.** Mammalian biochronology of the Arikareean through Hemphillian interval (late Oligocene through early Pliocene epochs). In: Woodburne MO, ed. *Late Cretaceous and Cenozoic mammals of North America: biostratigraphy and geochronology*. New York: Columbia University Press, 169–231.

Terry RC. 2004. Owl pellet taphonomy: a preliminary study of the post-regurgitation taphonomic history of pellets in a temperate forest. *Palaios* **19:** 497–506.

Thorington RW, **Schennum CE**, **Pappas LA**, **Pitassy D. 2005.** The difficulties of identifying flying squirrels (Sciuridae: Pteromyini) in the fossil record. *Journal of Vertebrate Paleontology* **25:** 950–961.

Wilson RL. 1968. Systematics and faunal analysis of a lower Pliocene vertebrate assemblage from Trego County, Kansas. *Contributions from the Museum of Paleontology University of Michigan* **22:** 75–126.

Zheng Y, **Wiens JJ. 2016.** Combining phylogenomic and supermatrix approaches, and a time-calibrated phylogeny for squamate reptiles (lizards and snakes) based on 52 genes and 4162 species. *Molecular Phylogenetics and Evolution* **94:** 537–547.

SUPPORTING INFORMATION

Additional Supporting Information may be found in the online version of this article at the publisher's web-site:

Table S1. Analysis statistics from parsimony analyses.
Figure S1. Selected computed tomography slices illustrating morphology of nasals. A, xy slice 239. B, xy slice 272. C, xy slice 448. Abbreviations: De, dentary; Mx, maxilla; Na, nasal; os, osteoderm; Px, premaxilla; Vo, vomer.
Figure S2. Computed tomography slice xy 1044, illustrating the presence of the free posteroventral margin of the intramandibular septum. Abbreviation: ims, intramandibular septum.
Figure S3. Majority rule consensus tree of Bayesian phylogenetic analysis of Gerrhonotinae with full scaffold.
Figure S4. Majority rule tree of Bayesian phylogenetic analysis of Gerrhonotinae with partial scaffold.
Figure S5. Majority rule tree of unconstrained Bayesian phylogenetic analysis of Gerrhonotinae.

Figure S6. Strict consensus tree of parsimony phylogenetic analysis of Gerrhonotinae with full scaffold.
Figure S7. Strict consensus tree of parsimony phylogenetic analysis of Gerrhonotinae with partial scaffold.
Figure S8. Strict consensus tree of unconstrained parsimony phylogenetic analysis of Gerrhonotinae.